

# Probing Isospin Dynamics in Halo Nuclei

H. Lenske, F. Hofmann and C.M. Keil

Institut für Theoretische Physik,  
Universität Giessen, D-35392 Giessen, Germany

## Abstract

Nuclear many-body theory is used to study nuclear matter and finite nuclei at extreme isospin. In-medium interactions in asymmetric nuclear matter are obtained from (Dirac-) Brueckner theory. Neutron skin formation in Ni and Sn isotopes is investigated by relativistic mean-field calculations in DDRH theory with density dependent meson-nucleon vertices. Applications to light nuclei are discussed with special emphasis on pairing and core polarization in weakly bound nuclei. Approaches accounting for continuum coupling in dripline pairing and core polarization are presented. Calculations for the halo nuclei  ${}^8\text{B}$ ,  ${}^{11}\text{Be}$  and  ${}^{19}\text{C}$  show that shell structures are dissolving when the driplines are approached. Relativistic breakup data are well described by eikonal calculations.

## 1 Introduction

Tremendous progress has been made over the last decade in extending our knowledge into hitherto unknown regions of the nuclear chart. The experimental achievements [1] were accompanied by complementary developments in nuclear theory. Nuclear structure physics has now access to nuclei with a large variety of proton-to-neutron ratios, hence allowing to study nuclear forces at extreme isospin. An equally important new aspect is the strong reduction in separation energies close to the driplines. Under such conditions the conventional binding mechanisms known from  $\beta$  stable nuclei are likely to cease to be valid. There are experimental indications - which are strongly supported by theory - that single particle shell structures become dissolved in the vicinity of proton and neutron driplines. If confirmed this observation will have important consequences because it means that the seemingly well-established prevalence of static mean-field dynamics is being replaced by dynamical processes from nucleon-nucleon (NN) interactions. In a very clean way this type of dynamics is observed in halo nuclei while in medium and heavy nuclei the dominance of the nuclear mean-field seems to survive. But with increasing neutron excess the character of the mean-field is dramatically changed by the strong enhancement of isovector interactions. For very neutron-rich nuclei theory predicts the formation of rather thick layers of almost pure neutron matter representing a genuine state of de-mixed proton and neutron fluids.

Descriptions of nuclear interactions and nuclei far off stability necessarily afford strong extrapolations. Since data are still scarce the theoretical calculations rely on nuclear models, to be justified (or falsified) by experiment. An approach attempting a self-contained description of stable and unstable nuclei by nuclear many-body theory is presented in the following sections.

## 2 Interactions in Strongly Asymmetric Matter

An appropriate approach to in-medium nuclear interactions is Brueckner theory. Especially the relativistic effects accounted for with Dirac-Brueckner (DB) calculations have proven to describe nuclear matter properties rather satisfactorily. In ref.[2] DB Hartree-Fock (DBHF) theory was used to investigate interactions in infinite matter over a large range of asymmetries. The Groningen free-space NN-potential was applied. Effective in-medium meson-nucleon coupling constants were extracted for the isoscalar  $\sigma$  and  $\omega$  and the isovector  $\rho$  and  $\delta$  mesons, respectively [2]. In all meson channels a pronounced dependence on the isoscalar bulk density is found while the dependence on the asymmetry is close to negligible.

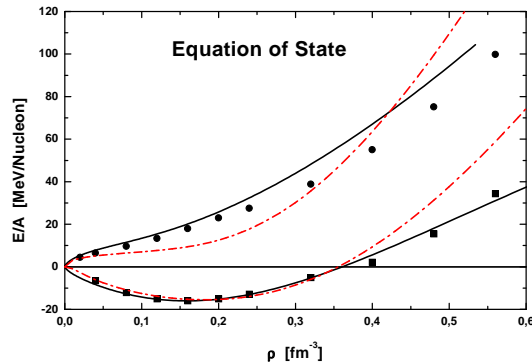


Figure 1: Equation of state for symmetric nuclear matter and neutron matter obtained with the D3Y interaction (full lines), the relativistic DDRH interaction [4] (dashed-dotted lines) and from variational calculations [8] (full squares and circles).

Hence, to a very good approximation in-medium strong interactions remain intrinsically independent of isospin thus conserving a fundamental symmetry. Using the density dependent relativistic hadron (DDRH) field theory [3] the DB coupling constants have been applied to finite nuclei [4], hypernuclei [5] and neutron stars [6]. DDRH theory is a microscopic formulation of relativistic mean-field theory [7] but describing in-medium effects by density dependent coupling constants rather than by non-linear meson self-interactions. The DDRH calculations describe binding energies, separation energies and other ground state properties of stable and unstable nuclei rather accurately on a level of a few percent [4] showing that the gross properties of nuclear matter and finite nuclei are described very satisfactorily with microscopic interactions.

A clear indication for the incompleteness of a ladder-type interaction model is found in a re-analysis of the DDRH results with a mass-formula showing that especially surface energy contributions are underestimated [4]. An important class of interactions not accounted for by DB theory are contributions from ring-diagrams which will become important at low densities. Also missing are three-body interactions [8]. In order to account for the missing contributions we follow the approach of [10] and introduce a semi-microscopic effective interaction by multiplying the Brueckner results by an additional density dependent vertex functional where parameters are fixed in symmetric matter. Results for the equation of state of symmetric and pure neutron matter obtained with DDRH theory are displayed in Fig.1 and compared to the non-relativistic density dependent D3Y parameterization [10].

An interesting effect, predicted by many mean-field models, is the appearance of neutron- and proton-skins when the driplines are approached. In Fig.2 DDRH proton and neutron density distributions for the isotopic chains of  $^{48-82}\text{Ni}$  and  $^{100-140}\text{Sn}$  nuclides are displayed [4]. At the proton dripline ( $^{48}\text{Ni}$ ,  $^{100}\text{Sn}$ ) proton skins are found being mainly caused by the Coulomb repulsion. With increasing neutron excess neutron skins starts to develop which, for example in the Ni-case, reach a thickness of about  $\Delta = 0.8$  fm at the neutron dripline, obtained here for  $^{92}\text{Ni}$ . In skin nuclei a core of normal composition is coated by a layer of almost pure neutron matter. Investigation of this very particular state of nuclear matter by transfer reactions at REX-ISOLDE energies is discussed in [9].

In most of the following calculations for dripline nuclei non-relativistic HFB and RPA (or QRPA) theory will be used. The main reason for doing so is that at present the extension of DDRH theory (as is also true for phenomenological RMF models) to a full dynamical description is still in progress. Relativistic interactions are well tested at the level of HF and HFB theory, i.e. in the limit of a static ground state calculations in the *no-sea* approximation. But only few is known about extensions to dynamical processes, which in a relativistic approach should take into account also the coupling to vacuum modes.

The non-relativistic D3Y interaction is based on a parameterization of the G-Matrix in terms of boson exchange interactions, including  $\pi$ ,  $\sigma$ ,  $\omega$  and  $\rho$  exchange. Because of the known inability of non-

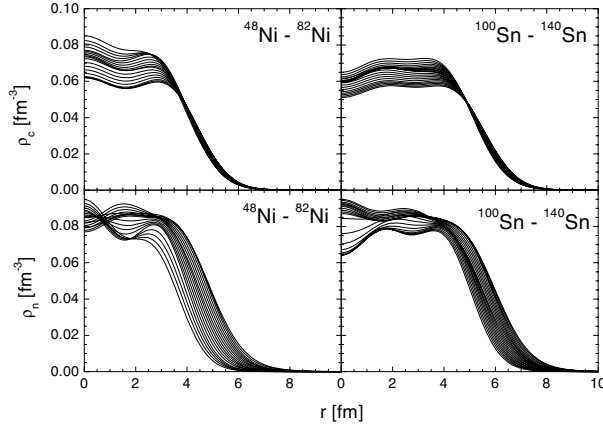


Figure 2: Charge densities (upper panel) and neutron ground state density distributions (lower panel) for Ni- and Sn-isotopes [4]. The formation of neutron skins in the neutron-rich nuclides is clearly visible.

relativistic Brueckner theory to reproduce adequately the empirical nuclear matter EoS an additional density dependent re-scaling was introduced in the *particle-hole* (*ph*) channel, enforcing agreement with the variational EoS of ref.[8] of for symmetric nuclear matter. Using Landau-Migdal theory [12] the appropriate (density dependent) *ph* interactions in the various spin and isospin channels are derived self-consistently.

### 3 Pairing at the Particle Threshold

The existence of  $^{11}\text{Li}$  as a particle-stable system relies almost completely on the mutual interactions among the last two valence neutrons. Their low separation energy,  $S_{2n}=320$  keV, points to the importance of the mixing with unbound states. For a detailed description of the valence wave function the conventional BCS and HFB methods using representations in terms of mean-field wave functions are not suitable. Theoretically, continuum effects are properly described by solving the Gorkov-equations [13]

$$(h - e_+) \Phi_+ - \Delta \Phi_- = 0 \quad , \quad (h - e_-) \Phi_- + \Delta \Phi_+ = 0 \quad (1)$$

as coupled equations for the hole and particle components [14] which are denoted by  $\Phi_{\pm}$  and are coupled by the pairing field  $\Delta$ . The single particle energies are  $e_{\pm} = \lambda \pm E$  where  $\lambda$  and  $E$  ( $\geq 0$ ) are the chemical potential and the quasiparticle energy, respectively. Note, that  $e_{\pm}$  will in general *not* coincide with the eigenvalues of the mean-field Hamiltonian  $h$ . In this sense, the states  $\Phi_{\pm}$  are off the (mean-field) energy shell and deviate from usual quasiparticle picture.

A necessary condition for particle-stability is  $\lambda < 0$ . Then, irrespective of the value of  $E$ , the hole-type solutions  $\Phi_-$  are exponentially decaying for  $r \rightarrow \infty$ . For  $E \leq |\lambda|$ , an exponential asymptotic behaviour is also found for the particle-type components  $\Phi_+$  and a discrete subset of eigenvalues  $E$  is obtained. For  $E > |\lambda|$ , eq.(1) has to be solved with continuum wave boundary conditions for  $\Phi_+$  leading to single particle spectral functions being distributed continuously in energy. Hence the quasi-particle picture, underlying BCS theory and, to some degree, also discretized HFB theory, is extended to a fully dynamical continuum description.

Here, we consider only like-particle ( $S = 0, T = 1$ ) pairing. Writing for protons ( $q = p$ ) and neutrons ( $q = n$ )  $\Phi_+(r, e_+) = u_q(e_+) F_q(r, e_+)$  and  $\Phi_-(r, e_-) = v_q(e_-) G_q(r; e_-)$ , respectively, where the reduced wave functions  $F_q$  and  $G_q$  are normalized to unity and  $u_q, v_q$  correspond to BCS amplitudes, the pairing fields are then defined in terms of the anomalous or pairing density matrices for protons and neutrons, respectively,

$$\kappa_q(r_1, r_2) = \frac{1}{2} \sum \frac{2j+1}{4\pi} \int_0^\infty dE u_{qj\ell}(E) v_{qj\ell}(E) F_{qj\ell}(r_1, E) G_{qj\ell}(r_1, E) \quad (2)$$

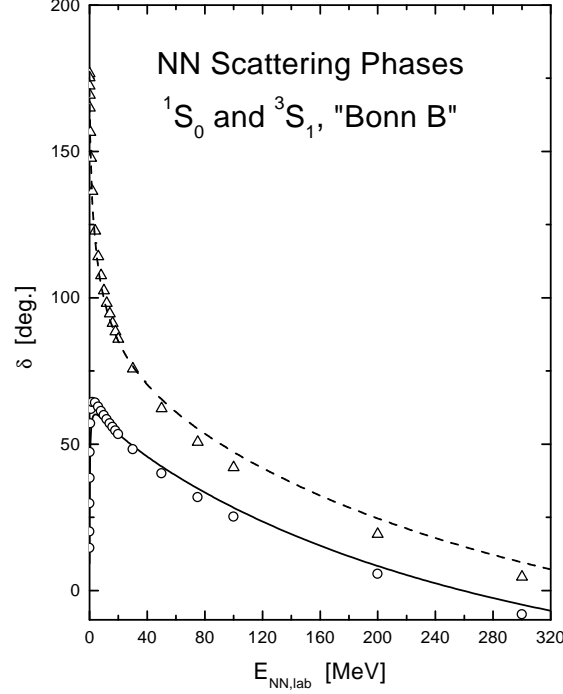


Figure 3: Singlet-Even ( $^1S_0$ , full line) and Triplet-Even ( $^3S_1$ , dashed line) S-wave phase shifts obtained with the D3Y-interaction in free space are compared to calculations with the Bonn-B NN potential (circles and triangles) [16].

and the proton and neutron pairing fields are

$$\Delta_q(r_1, r_2) = V_{SE}(r_1, r_2)\kappa_q(r_1, r_2) \quad . \quad (3)$$

If  $\lambda < 0$ ,  $\kappa_q(r)$  and  $\Delta(r)$  are guaranteed to decay exponentially for  $r \rightarrow \infty$ . The pairing interaction in the *particle – particle* channel is described by  $V_{SE}$ . It is still an open question whether the free space or an in-medium singlet-even interaction should be used (see e.g. [15]).

Here, for the numerical calculations a local momentum approximation is introduced by averaging in momentum space over the non-locality and replacing  $V_{SE}(r_1, r_2) \rightarrow M_{SE}(k_F(r))\delta(r_1 - r_2)$ . This corresponds to including the off-shell correlations into the strength factor  $M_{SE}$  which, as a consequence, acquires an intrinsic density dependence. It is given by the in-medium on-shell *SE* scattering amplitude at the local on-shell momentum  $k_F(r)$ , i.e. the (two-body) S-wave component of the *SE* Brueckner G-matrix in the *particle – particle* channel. The density dependence is re-adjusted such that for  $\rho \rightarrow 0$  the free space *SE* S-wave phase shifts are reproduced. A comparison to the Bonn-B phase shifts [16] is shown in Fig.3.

In order to understand pairing in weakly bound nuclei in more detail it is instructive to extract from eq.(1) (non-local and energy-dependent) dynamical pairing self-energies in the particle and hole channel, respectively,

$$\Sigma_{\pm}(1, 2; \omega) = \Delta(1)^{\dagger} g_{\mp}(1, 2; \omega) \Delta(2) \quad , \quad (4)$$

where  $g_{\pm}(1, 2; \omega)$  is the mean-field single particle propagator in the complementary (hole or particle) channel. This leads to the equivalent set of (formally) decoupled integro-differential equations

$$(h(1) - e_1 + \int d2 \Sigma_{+}(1, 2; E)) \Phi_{+} = 0 \quad , \quad (h(1) - e_1 + \int d2 \Sigma_{-}(1, 2; E)) \Phi_{-} = 0 \quad (5)$$

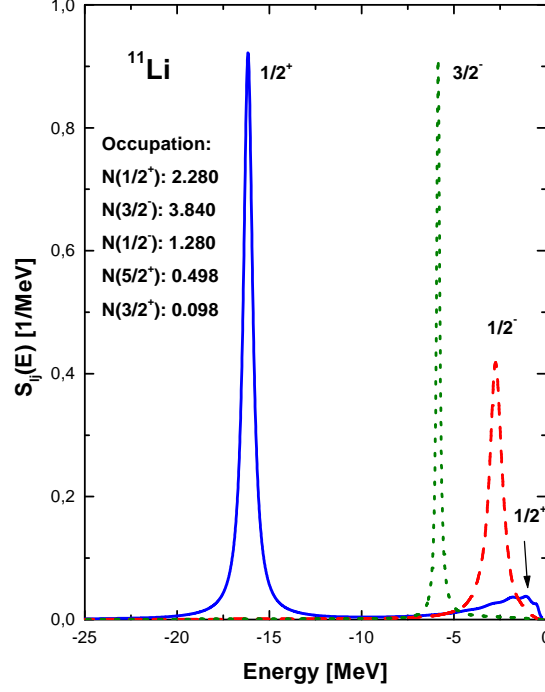


Figure 4: Single particle spectral functions for s- and p-wave neutron states in  $^{11}\text{Li}$ . The finite widths of the states is due to continuum coupling. The partial occupation numbers  $N_{j\ell}$  are also shown, including d-wave contributions.

showing that the generalized pairing approach may depart strongly from a conventional BCS description, especially when  $\Sigma_{\pm} \sim \mathcal{O}(e_{\pm})$  becomes comparable in magnitude to the effective single particle energies  $e_{\pm}$ . In the constant-gap BCS approximation  $\Delta(r) \rightarrow -\Delta_0$  the self-energies become

$$\Sigma_{+}^{BCS} = -\Delta_0 \frac{v_{j\ell}}{u_{j\ell}} \quad ; \quad \Sigma_{-}^{BCS} = -\Delta_0 \frac{u_{j\ell}}{v_{j\ell}} \quad (6)$$

and eq.(5) reduces to the conventional BCS eigenvalue problem.

Returning to the full problem, strength functions for  $^{11}\text{Li}$  are displayed in Fig.4. The strong deviation from a pure mean-field or BCS description is apparent by observing that besides the expected s- and p-wave components also  $d_{5/2,3/2}$  strength is lowered into the bound state region. Remarkably, the mean-field does not support neither bound  $2s$  nor  $1d_{5/2,3/2}$  single particle levels and their appearance is solely due to pairing. The states acquire a finite width because of the coupling to the particle continuum.

Theoretically, the proton ( $q = p$ ) and neutron ( $q = n$ ) densities in a systems like  $^{11}\text{Li}$  are defined by

$$\rho_q(r) = \sum_{j\ell} \frac{2j+1}{4\pi} \int_{-\infty}^{\lambda} de_{-} v_{qj\ell}^2(e_{-}) |G_{qj\ell}(r, e_{-})|^2 \quad , \quad (7)$$

from which the particle numbers

$$N_q = \sum_{j\ell} (2j+1) \int_{-\infty}^{\lambda} de_{-} v_{qj\ell}^2(e_{-}) = \sum_{j\ell} (2j+1) n_{qj\ell} \quad , \quad (8)$$

are found. The neutron partial wave occupation numbers  $N_{j\ell} = (2j+1)n_{j\ell}$  are included in Fig.4. In stable nuclei discrete levels at  $2\lambda < e_{-} < \lambda$  will contribute to eq.(7). In extreme drip-line nuclei they

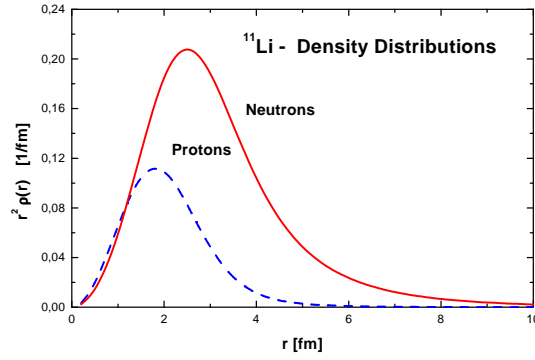


Figure 5: Proton and neutron ground state density distributions (weighted by  $r^2$ ) for  $^{11}\text{Li}$ . The strong neutron halo component formed by s-,p- and d-states is clearly visible.

are missing because of the smallness of  $|\lambda|$ . In Fig.5 the proton and neutron ground state densities are shown, multiplied by  $r^2$  in order to emphasize the differences in shape and the neutron halo component. Applications of the densities in high-energy elastic scattering of  $^{11}\text{Li}$  on a proton target are discussed in [17]. Measured  $^{11}\text{Li}$  response functions were analyzed by QRPA calculations in [18].

Rather than solving the full continuum pairing problem as discussed here a widely used approach is to represent the Gorkov spectrum by a set of discretized energy levels by imposing a box boundary condition on the solutions of eq.(1) [15]. A comparison shows a good agreement between the full and the discretized calculations for binding energies, chemical potentials and ground state densities provided the box radius is chosen large enough ( $R_{box} \geq 50\text{fm}$ ).

## 4 Dynamical Core Polarization at the Dripline

Dynamical core polarization is seen most clearly in nuclei with a single nucleon outside a core. Approaching the driplines the core nucleus by itself is already far off stability containing weakly bound single particle orbits. Under these circumstances the surface tension and therefore the restoring forces against external perturbations are reduced. Such "soft core" systems are, for example, found in the neutron-rich even-mass carbon isotopes. A good indicator is the existence of low-energy  $2^+$  states, decreasing in energy with increasing mass. Continuum QRPA calculations with a residual interaction derived in Landau-Fermi liquid theory from the D3Y in-medium interaction reproduce the systematics of  $2^+$  states rather well. This leads to the conclusion that they are mainly of vibrational nature rather than due to static deformation as assumed e.g. in [25].

The calculations predict a strong increase of the quadrupole polarizabilities in the carbon isotopes for increasing neutron excess with a maximum around  $^{16,18}\text{C}$ . This behaviour is due to the lowering of the first  $2^+$  state which in  $^{12}\text{C}$  is located at  $E_x = 4.44\text{ MeV}$  and moves down to  $E_x = 1.66\text{ MeV}$  in  $^{18}\text{C}$ . The dipole (or electric) polarizability, however, changes only within 10% over the  $^{10-22}\text{C}$  isotopic chain.

In a system with core polarization the valence particle (or hole) obeys a non-static wave equation

$$(H_{MF} + \Sigma_{pol}(\varepsilon) - \varepsilon) \Psi = 0 \quad (9)$$

including the static (HFB) mean-field Hamiltonian  $H_{MF}$  and the non-local and energy-dependent polarization self-energy  $\Sigma_{pol}$  describing the rescattering of the nucleon off the core thereby exciting it into states of various multipolarities and excitation energies followed by subsequent de-excitations back to the ground state (see Fig.6).

During these processes the particle can be scattered virtually into high lying orbitals. The quantum numbers of the intermediate  $2p1h$  (or  $1p2h$ ) configurations are only constraint by the requirement that spin and parity much match those of the leading particle configuration, given by the state moving with

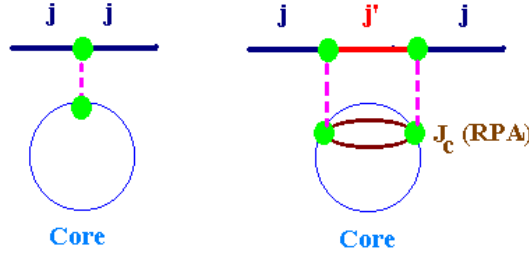


Figure 6: Diagrammatic structure of mean-field (left) and core polarization interactions (right) of a nucleon in single particle state  $j$ . Interactions (meson exchange) are indicated by dashed lines. Core polarization leads to intermediate states ( $j'J_c$ ) with a (QRPA) core excitation  $J_c$  and a single particle state  $j'$ .

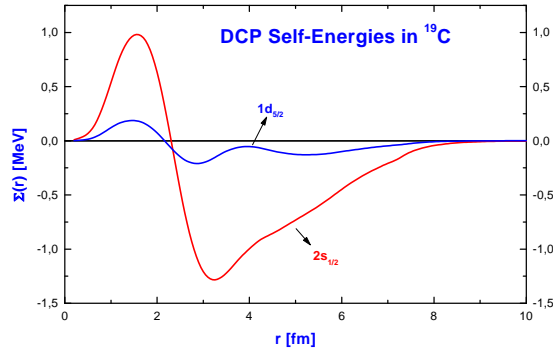


Figure 7: Core polarization self-energies for low energy  $^{19}\text{C}(1/2^+)$  and  $^{19}\text{C}(5/2^+)$  states. Only the local parts ( $r = r_1 = r_2$ ) are shown.

respect to the inert core in its ground state. In nuclear matter and finite nuclei these processes are known to give rise to a depletion of momentum space ground state occupation probabilities [20, 21] from the step function momentum distribution of a Fermi gas of quasiparticles interacting only by a static mean-field. In practice, the core excitations are calculated in QRPA theory thus extending the static HFB picture in a consistent way to a dynamical theory.

In a finite nucleus the dynamical single particle self-energies  $\Sigma_{pol}$  affect separation energies and wave functions. In dripline nuclei the polarization self-energies are found to have a pronounced state-dependence. In Fig.7 DCP self-energies for the lowest  $1/2^+$  and  $5/2^+$  in  $^{19}\text{C}$  are shown. In the  $5/2^+$  channel the overall strength is small and a fluctuating shape is obtained. The  $1/2^+$  states, however, experience an additional attraction from an attractive surface-type self-energy which, in fact, provides the main source of binding for  $^{19}\text{C}(1/2^+, g.s.)$ .

Theoretically, this amounts to use a multi-configuration ground state containing a single particle component - reminiscent of the static mean-field configuration - and a multitude of configurations where the valence particle is rescattered into other orbits by interactions with the core [14, 19]. Coupling to the lowest  $2^+$  and  $3^-$  states only as advocated e.g. in [26] cannot account for the complexity of the process.

Results for energies and spectroscopic factors in the single neutron halo nuclei  $^{11}\text{Be}$  and  $^{19}\text{C}$  and the single proton halo nucleus  $^8\text{B}$  [22] are shown in Tab.1. In  $^{11}\text{Be}$  core polarization is causing the reversal of  $1/2^+$  and  $1/2^-$  states by supplying an additional attractive self-energy in the  $1/2^+$  channel. The single particle spectroscopic factor  $S_n(1/2^+, g.s.)=0.75$  is in good agreement with recent transfer and breakup data. A more dramatic effect is found in  $^{19}\text{C}$  and also  $^{17}\text{C}$  where the g.s. components

Table 1: Energies, spins and ground state spectroscopic factors from core polarization calculations.

<i>Nucleus</i>	$j^\pi$	<i>Energy keV</i>	$S(j^\pi, g.s.)$
${}^8B$	$3/2^-$	130	0.73
${}^{11}Be$	$1/2^+$	510	0.74
${}^{17}C$	$5/2^+$	760	0.51
${}_{s}{}^{19}C$	$1/2^+$	263	0.41

Table 2: Theoretical one-nucleon removal cross section on a  ${}^{12}C$  target and width of the calculated momentum distributions obtained with core-polarized wave functions and eikonal reaction calculations are compared to data [24]. One-proton and one-neutron removal reactions are indicated by (-1p) and (-1n), respectively.

<i>Isotope</i>	<i>Energy</i>	$\sigma_{-1N}$	<i>FWHM</i>	$\sigma_{-1N}^{exp}$	<i>FWHM<sup>exp</sup></i>
	<i>MeV/nucleon</i>	<i>mb</i>	<i>MeV/c</i>	<i>mb</i>	<i>MeV/c</i>
${}^8B (-1p)$	1440	104	75	$98 \pm 6$	$91 \pm 5$
${}^{10}B (-1p)$	1450	17.3	145	$17 \pm 2$	$165 \pm 8$
${}^{17}C (-1n)$	904	124	132	$129 \pm 22$	$143 \pm 5$
${}^{19}C (-1n)$	910	192	69	$233 \pm 51$	$68 \pm 3$

are strongly suppressed as seen from the small spectroscopic factors in Tab.1. Hence, the valence nucleon is no longer attached to a definite mean-field orbital but exists in a wave packet-like state spread over a certain range of shell model states. In other words, mean-field dynamics have ceased to be the dominant source of binding. Rather, the  ${}^{17}C$  and  ${}^{19}C$  results indicate a new type of binding mechanism in dripline nuclei where shell structures are dissolved and binding is obtained from dynamical valence-core interactions.

Core polarization also affects the low energy continuum region of dripline nuclei. The admixtures of core excitations may give rise to configurations where neither of the involved nucleons is in a state above threshold although the total energy is well above particle threshold. Such states are known as *bound states embedded in the continuum* (BSEC). They decay by coupling to energetically degenerate single particle continuum states. A known case is a  $3/2^+$  state in  ${}^{13}C$  which was predicted in [27] and observed experimentally [28]. In  ${}^{19}C$  BSEC-type configurations are indeed found in the s-, p- and d-wave channels below about 6 MeV above neutron threshold. They appear as resonances in the continuum strength functions. In Fig.8  ${}^{19}C(1/2^+)$  and  ${}^{19}C(5/2^+)$  DCP continuum spectral functions are shown. The BSEC structures are most prominent in the  $1/2^+$  channel because the missing potential barrier will not support potential resonances. In other words, observing a  $1/2^+$  resonance is a direct proof for a state with a non-trivial many-body structure. The  $5/2^+$  state seen in Fig.8 is part of a (much broader) conventional d-wave potential resonance being shifted into the low energy region by core interactions. Clearly, the existence of such close-to-threshold BSEC states will have important consequences for breakup reactions and, especially, for neutron capture in astrophysical processes.

The theoretical overlap wave functions have been used in eikonal breakup calculations at relativistic energies. The FRS/GSI data for longitudinal momentum distributions [22, 23] and removal cross sections [24] are well described as seen from Table 2.

## 5 Summary

Nuclear many-body theory was applied to strongly asymmetric nuclear matter and the ground and excited states of dripline nuclei. Interactions were derived from Brueckner and Dirac-Brueckner calculations supplemented by additional density dependences accounting for interaction contributions which



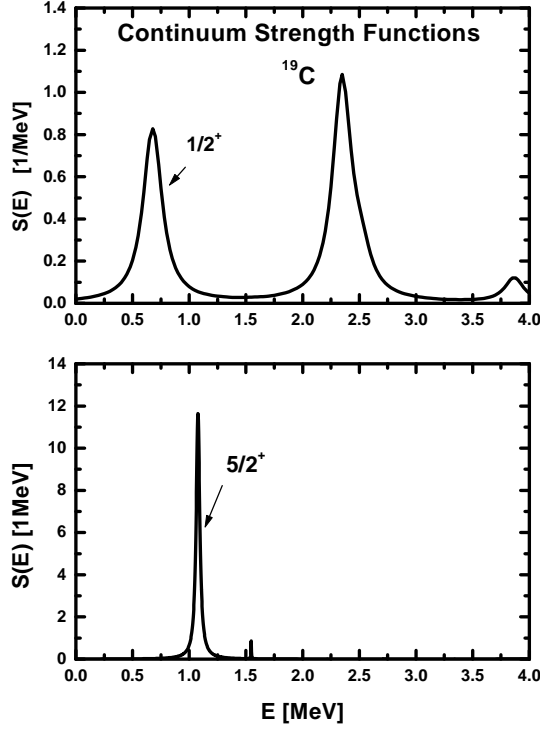


Figure 8: Continuum strength functions for  $^{19}\text{C}(1/2^+)$  (upper panel) and  $^{19}\text{C}(5/2^+)$  (lower panel). BSEC-like resonance structures are seen, especially in  $1/2^+$  channel.

are not contained in the ladder approach. Pairing in weakly bound system was described in a approach taking into account the coupling to unbound continuum configurations. Dynamical core polarization in single nucleon halo systems was investigated by HFB and QRPA methods, also accounting for continuum effects.

The overall features of dripline nuclei are rather well described. However, open and interesting questions remain on the structure of interactions especially in the low-density region. Here, the present treatment of interactions lacks full self-consistency by the semi-empirical adjustments to variational results. Especially three-body interactions and induced 2-body interactions from ring diagrams in weakly bound asymmetric nuclear matter and finite nuclei have to be investigated further. Experimentally, this could be complemented by high-resolution measurements of spectral functions in the bound and the continuum region.

The calculations strongly emphasize the importance of continuum coupling. They are found to dissolve shell structures close to the driplines and create BSEC structures in the low energy continuum. It will be interesting to investigate core polarization and continuum pairing for transfer and breakup reactions and capture reactions in astrophysical scenarios.

## Acknowledgments

This work is supported in part by DFG (contract Le439/4), GSI Darmstadt and BMBF. Inspiring collaborations with the GSI/FRS nuclear structure groups and G. Schrieder, TU Darmstadt, are gratefully acknowledged.

## References

- [1] P.G. Hansen, A.S. Jensen, B. Jonson, *Ann. Rev. Phys. Sci. (N.Y.)* 45 (1995) 591 .
- [2] F. de Jong, H. Lenske, *Phys. Rev. C* 57 (1998) 3099 .
- [3] H. Lenske, F. Fuchs, *Phys. Lett. B* 345 (1995) 355 ; C. Fuchs, H. Lenske, H. Wolter, *Phys. Rev. C* 52 (1995) 3043 .
- [4] F. Hofmann, C. Keil, H. Lenske, *Phys. Rev. C* (in print) ; nucl-th/0007050.
- [5] C. Keil, F. Hofmann, H. Lenske, *Phys. Rev. C* 61 (2000) 06401 .
- [6] F. Hofmann, C. Keil, H. Lenske, *Phys. Rev. C* (submitted) ; nucl-th/0008038.
- [7] P. Ring, *et al.*, *Ann. Phys. (N.Y.)* 198 (1990) 132 .
- [8] V.J. Pandharipande *et al.*, *Phys. Rev. C* 58 (1998) 1804 .
- [9] H. Lenske, G. Schrieder, *Euro. Phys. J. A* 2 (1998) 41 ; C. Gund *et al.*, *Euro. Phys. J. A* (in print), see nucl-ex/0010005.
- [10] F. Hofmann, H. Lenske, *Phys. Rev. C* 57 (1998) 183 .
- [11] E. Chabanat *et al.*, *Nucl. Phys. A* 627 (1997) 273 .
- [12] F.T. Baker *et al.*, *Phys. Rep.* 289 (1997) 235 .
- [13] L.P. Gorkov, *JETP* 9 (1959) 1364 ; see also [15].
- [14] H. Lenske, *J. Phys. G* 24 (1998) 1429 .
- [15] see e.g. W. Nazarewicz, these proceedings; P.Ring, *ibid.*.
- [16] R. Machleidt, *Adv. Nucl. Phys. (N.Y.)* 19 (1989) 189 .
- [17] P. Egelhoff, these proceedings.
- [18] M. Zinser, H. Emling, H. Lenske *et al.*, *Nucl. Phys. A* 619 (1997) 151 .
- [19] F.J. Eckle *et al.*, *Phys. Rev. C* 39 (1989) 1662 and *Nucl. Phys. A* 506 (1990) 199 .
- [20] F. de Jong, H. Lenske, *Phys. Rev. C* 54 (1996) 1488 .
- [21] J. Lehr *et al.*, *Phys. Lett. B* 483 (2000) 324 .
- [22] M.H. Smedberg *et al.*, *Phys. Lett. B* 452 (1999) 1 .
- [23] T. Baumann *et al.*, *Phys. Lett. B* 439 (1998) 256 .
- [24] D. Cortina-Gil *et al.*, *Euro. Phys. J. A* (in print) .
- [25] F. Nunes *et al.*, *Nucl. Phys. A* 596 (1996) 171 .
- [26] N. Vinh-Mau, *Nucl. Phys. A* 592 (1995) 33 .
- [27] G. Baur and H. Lenske, *Nucl. Phys. A* 282 (1977) 201 .
- [28] H. Fuchs *et al.*, *Nucl. Phys. A* 343 (1980) 133 .